

Generating single- and many-body quantum magnonic states

V. Williams,^{1,*} J. M. P. Nair,^{1,†} Y. Tserkovnyak,^{2,‡} and B. Flebus^{1,§}

¹*Department of Physics, Boston College, 140 Commonwealth Avenue, Chestnut Hill, Massachusetts 02467, USA*

²*Department of Physics and Astronomy and Bhaumik Institute for Theoretical Physics,
University of California, Los Angeles, California 90095, USA*

(Dated: August 4, 2025)

The growing interest in quantum magnonics is driving the development of advanced techniques for generating, controlling, and detecting non-classical magnonic states. Here, we explore the potential of an ensemble of solid-state spin defects coupled to a shared magnetic bath as a source of such states. We establish a theoretical framework to characterize the quantum correlations among magnons emitted by the ensemble into the bath and investigate how these correlations depend on experimentally tunable parameters. Our findings show that the emitted magnons retain the quantum correlations inherent to the solid-state emitters, paving the way for the deterministic generation of quantum many-body magnonic states.

Introduction.—Although still in its infancy, the field of quantum magnonics has recently gained momentum, driven by its potential to advance quantum technologies [1–3]. This growing interest is fueled by the unique and versatile properties of magnons, i.e., the quantized excitations of spin waves in magnetically ordered materials [4]. Their broad tunability, intrinsic non-reciprocities, and seamless integration with established quantum platforms make them promising candidates for applications ranging from quantum information processing to scalable quantum communication networks. Central to the advancement of this field is the ability to generate, manipulate, and detect quantum magnon states, which would enable the encoding, transfer, and processing of information within hybrid quantum circuits [5, 6] and serve as building blocks for continuous-variable quantum information processing [1, 7]. Recent breakthroughs in encoding and transmitting information using magnons have inspired several theoretical proposals for generating single-magnon quantum states, most of which focus on enhancing the nonlinearities within magnonic systems such as magnon blockades [8–14], and parametric pumping [7, 15].

In this Letter, we explore an alternative route for sourcing single magnon states that can also, more intriguingly, enable the generation of quantum many-body magnonic states. Our approach – schematically illustrated in Fig. 1 – relies on the well-established interaction between solid-state spin defects and the magnetic noise emitted by a nearby magnetic system. This qubit-bath coupling is routinely leveraged in quantum sensing experiments, which probe the properties of a magnetic system via their effect on the sensor spin’s relaxation time [16, 17]. Quantum sensing experiments

are typically conducted by setting the resonance frequency ω of the solid-state spin defect above the magnetic system’s spin-wave gap Δ_F to maximize sensor-probe coupling strength. In this regime, i.e., $\hbar\omega > \Delta_F$, the solid-state spin defect can emit (absorb) magnons with energy $\hbar\omega$ into (or from) the magnetic bath, a process that can significantly shorten the spin defect’s relaxation time. To further enhance the noise produced by thermal spin-wave fluctuations, the operating temperature T is usually high enough to ensure a substantial thermal magnon population in the bath, i.e., $\Delta_F \ll k_B T$.

The regime of interest to this work is instead the quantum one, i.e., $T \rightarrow 0$, corresponding to essentially no thermal magnons available for absorption by a spin defect. In this scenario, if the spin defect is initialized in the excited state, its interaction with the magnetic system will eventually lead to the emission

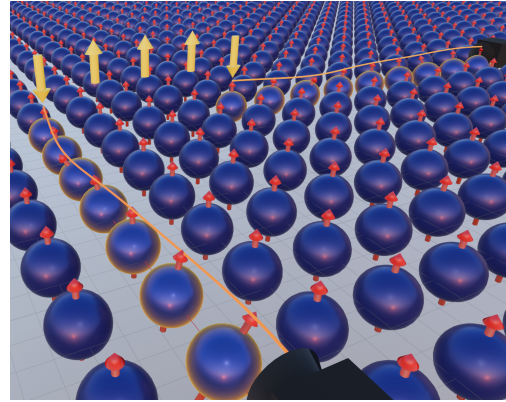


FIG. 1. Generation of quantum-correlated magnonic states via spontaneous emission from an ensemble of solid-state defects coupled to a common ferromagnetic bath. The blue square lattice represents the magnet, with red arrows indicating ground-state spin polarization. Upon transitioning from the excited to the ground state, the solid-state spin defect (yellow arrows) emit a spin wave (orange line) into the magnetic bath, which is subsequently probed by the detectors (black camera icons).

* willibte@bc.edu

† muttathi@bc.edu

‡ yaroslav@physics.ucla.edu

§ flebus@bc.edu

of a *single magnon* – a process that, to our knowledge, remains unexplored as a pathway for generating quantum magnonic states. Our goal is to build upon this potential of individual or uncorrelated solid-state spin defects as sources of single magnons to investigate the generation of quantum many-body magnonic states through ensembles of quantum-correlated solid-state spin defects. A theoretical foundation for our exploration is provided by the recent work of Li and co-authors [18], which has shown that the spontaneous emission of magnons into a common bath by an ensemble of solid-state spin defects can establish quantum correlations among them. These quantum correlations are at the source of cooperative quantum phenomena analogous to those observed in light-matter platforms [19–26], characterized by the formation of super- and sub-radiant states in the ensemble’s spontaneous emission. As shown by Refs. [21, 27], in light-matter interfaces collective relaxation dynamics generate correlations among qubits, which are subsequently imprinted onto the photons they emit. It is thus natural to ask whether this transfer of correlations from a qubit ensemble to emitted quasi-particles takes place also in the quantum hybrid spin platform depicted in Fig. 1, and whether it could be leveraged to enable the tunable generation of non-classical magnonic states. Here, we address this question by developing a general framework to describe the correlations of the magnons emitted by an ensemble of solid-state spin defects interacting with a magnetic bath. Our results reveal that quantum correlations within the many-body dynamics of the array result in directionally-correlated magnon emissions, opening avenues for controlled generation and detection of many-body quantum magnonic states.

Model.—We begin by introducing the theoretical toolbox that describes the dynamics of an ensemble of solid-state spin defects interacting via the spin-wave fluctuations of a common ferromagnetic film. For concreteness, we consider a $1d$ array oriented along the \hat{x} axis, with lattice constant a_q , of N identical spins polarized along the \hat{z} axis. Our framework is applicable to a wide range of solid-state spin defects. For instance, while a nitrogen-vacancy (NV) center forms a spin-triplet system for low energies, at low temperatures and in the presence of a magnetic field $\mathbf{B}_0 = B_0\hat{z}$, it can be treated as an effective two-level system with frequency $\omega = \Delta_0 - \tilde{\gamma}B_0$ in the $\{|0\rangle, |-1\rangle\}$ subspace, where Δ_0 is the NV center zero-field splitting and $\tilde{\gamma} > 0$ (minus) its gyromagnetic ratio [18]. The array is placed at a height d above a ferromagnetic film whose equilibrium spin density $\mathbf{s}(\boldsymbol{\rho})$ is aligned along the \hat{z} direction, i.e., $\mathbf{s} = (s_x, s_y, s)$, with $|\mathbf{s}| \simeq s$, with s being the saturation spin density. The fluctuations of the spin density around its equilibrium direction generate a magnetostatic field $\mathbf{B}_\alpha = \int d\rho \mathcal{D}(\rho_\alpha, \boldsymbol{\rho}, d)\mathbf{s}(\boldsymbol{\rho})$ where \mathcal{D} is the tensorial magnetostatic Green’s function of the magnetic dipolar

field [28]. The Hamiltonian of the array can then be written as

$$\mathcal{H} = \mathcal{H}_s + \mathcal{H}_{\text{int}}, \quad \text{with } \mathcal{H}_s = -\frac{1}{2} \sum_{\alpha} \omega \sigma_{\alpha}^z, \\ \mathcal{H}_{\text{int}} = \tilde{\gamma} \sum_{\alpha} \left(\sqrt{2} B_{\alpha}^+ \sigma_{\alpha}^- + \sqrt{2} B_{\alpha}^- \sigma_{\alpha}^+ + B_{\alpha}^z \sigma_{\alpha}^z \right), \quad (1)$$

where $B_{\alpha}^{\pm} = B_{\alpha}^x \pm i B_{\alpha}^y$, $\sigma_{\alpha}^- = |0_{\alpha}\rangle\langle -1_{\alpha}|$ and $\sigma_{\alpha}^+ = |-1_{\alpha}\rangle\langle 0_{\alpha}|$, with σ_{α} labeling the quantum spin at the site ρ_{α} . After tracing out the magnonic degrees of freedom of the bath using a Born–Markov approximation [23, 25, 26, 29], one finds that, in the vanishing temperature limit, i.e., $T \rightarrow 0$, the evolution of the density matrix ρ of the array can be written as ¹

$$\frac{d\rho}{dt} = -i \left[\mathcal{H}_s + \sum_{\alpha \neq \beta} (J_{\alpha\beta} \sigma_{\alpha}^+ \sigma_{\beta}^-), \rho \right] \\ + \sum_{\alpha\beta} \Gamma_{\alpha\beta} \left(\sigma_{\beta}^- \rho \sigma_{\alpha}^+ - \frac{1}{2} \{ \sigma_{\alpha}^+ \sigma_{\beta}^-, \rho \} \right). \quad (2)$$

Here, the term $\propto J_{\alpha\beta}$ represents a coherent exchange interaction that does not play a substantial role in our discussion as it is magnon number-conserving. The term $\propto \Gamma_{\alpha\beta}$, instead, describes dissipative processes, i.e., the emission of magnons into the ferromagnetic reservoir. For an array of non-interacting spins, the matrix $\Gamma = (\Gamma_{\alpha\beta})$ becomes diagonal, with entry $\Gamma_{\alpha\alpha} = \Gamma_0$ corresponding to the relaxation rate of the isolated α th spin. On the other hand, dissipative inter-qubit correlations result in finite off-diagonal terms $\Gamma_{\alpha\beta}$ that drive the correlated magnon emission and the ensuing cooperative quantum dynamics [18].

The explicit form of the matrix Γ depends on the spin susceptibility χ of the magnetic film [18, 21, 30, 31], which parameterizes its linear response to an external field \mathbf{h} . When $\hbar\omega > \Delta_F$, the main drive of correlated emission is the transverse magnetic noise encoded in the spin susceptibility χ^{+-} [18, 32], which is defined through

$$s^+(\boldsymbol{\rho}, t) = \gamma \int d\rho' dt' \chi^{+-}(\boldsymbol{\rho} - \boldsymbol{\rho}', t - t') h^+(\boldsymbol{\rho}', t'). \quad (3)$$

Here, γ is the gyromagnetic ratio of the film, and $s^{\pm} = (s^x \pm i s^y)/2$ and $h^{\pm} = h^x \pm i h^y$. In the long-wavelength limit, the transverse spin susceptibility can be extracted from the following Landau-Lifshitz-Gilbert (LLG) equation [33] :

$$\frac{d\mathbf{s}}{dt} = -\gamma \mathbf{s} \times \mathbf{B}_{\text{eff}} - \gamma \mathbf{s} \times \mathbf{h} + \frac{\alpha}{s} \mathbf{s} \times \frac{d\mathbf{s}}{dt}, \quad (4)$$

¹ For a detailed derivation see [18].

where $\alpha \ll 1$ is the dimensionless Gilbert damping parameter and $\mathbf{B}_{\text{eff}} = -\gamma^{-1} \partial \mathcal{H}_m / \partial \mathbf{s}$ is the effective (Landau-Lifshitz) field associated with the bath Hamiltonian. While Eq. (2) holds for a generic stationary ferromagnetic bath with reciprocal spin-wave dispersion, i.e., $\omega_{\text{F}}(\mathbf{k}) = \omega_{\text{F}}(-\mathbf{k})$ [34], we focus here for concreteness on a $U(1)$ -symmetric ferromagnet [18], whose Hamiltonian is given by

$$\mathcal{H}_m = \int d\rho \left[-Js(\rho) \cdot \nabla^2 \mathbf{s}(\rho) - As_z^2(\rho) + \gamma B_0 s_z(\rho) \right], \quad (5)$$

where J and A parametrize, respectively, a nearest-neighbor Heisenberg exchange interaction and a uniaxial anisotropy. Equation (5) describes a ferromagnet with spin-wave dispersion $\omega_{\text{F}}(k) = Dk^2 + \Delta_{\text{F}}$, where $D = sJ$ is the spin stiffness and $\Delta_{\text{F}} = K + \gamma B_0$, with $K = 2sA$, the spin-wave gap. Plugging Eq. (5) into Eq. (4), we obtain

$$\chi^{+-}(k, \omega) = \frac{s/2}{D(k^2 - 1/\lambda^2) + i\alpha\omega}, \quad (6)$$

where $\lambda = \sqrt{D/(\omega - \Delta_{\text{F}})}$ is the characteristic wavelength of the magnons emitted by the solid-state spin defects. Taking as an example an NV center ensemble interacting with a Yttrium Iron Garnet (YIG) film with spin stiffness $D = 5.1 \times 10^{-28}$ erg \cdot cm² and zero-field gap $K = 3.6 \times 10^{-18}$ erg, setting the external field to $B_0 \sim 40$ mT results in a characteristic wavelength $\lambda \sim 280$ nm that is much larger than the minimal NV-bath separation d achievable experimentally [18]. In this regime, i.e., $d \ll \lambda$, the coherent and dissipative inter-qubit couplings can be written as

$$J_{\alpha\beta}/\nu = -\frac{\pi}{2} \frac{\omega - \Delta_{\text{F}}}{\Delta_0} Y_0 \left(\frac{\rho_{\alpha\beta}}{\lambda} \right), \quad (7)$$

and

$$\Gamma_{\alpha\beta}/\nu = \pi \frac{\omega - \Delta_{\text{F}}}{\Delta_0} J_0 \left(\frac{\rho_{\alpha\beta}}{\lambda} \right), \quad (8)$$

with $\nu = \frac{\pi h^3 (\gamma \tilde{\gamma})^2 s \Delta_0}{D^2}$ [18]. Here, $\rho_{\alpha\beta}$ is the spatial separation between the α th and β th qubits, and J_0 (Y_0) is the 0th order Bessel function of the first (second) kind. By plugging Eqs. (7) and (8) into Eq. (2), one can calculate the relaxation dynamics of the NV-center ensemble for any given initial state.

Correlated emission.—In order to characterize the statistics of the magnons emitted by the qubit ensemble into the reservoir, one must first establish a metric for the detection of a single magnon. Drawing inspiration from the field of quantum optics [35], we introduce the normalized second-order correlation function

$$g^{(2)}(\rho, \rho', t, t') = \frac{\langle s^+(\rho, t) s^+(\rho', t') s^-(\rho, t) s^-(\rho', t') \rangle}{\langle s^+(\rho, t) s^-(\rho, t) \rangle \langle s^+(\rho', t') s^-(\rho', t') \rangle}. \quad (9)$$

In the following, we focus on correlations in the far-field limit, which allows us to rewrite $g^{(2)}(\rho, \rho', t, t') \Rightarrow g^{(2)}(\phi, \phi', t, t')$. Furthermore, for the stationary fields considered in this work, we can further simplify $g^{(2)}(\phi, \phi', t, t') \Rightarrow g^{(2)}(\phi, \phi', \tau, 0)$, with $\tau = t - t'$. By invoking the Holstein-Primakoff transformation, i.e., $s^+ \propto \sqrt{2s} a^\dagger$, where a^\dagger is the magnon creation operator, Eq. (9) can be understood as the joint probability of two simultaneous magnon emissions normalized by their independent probabilities. In analogy with its quantum optical counterpart [36, 37], it characterizes the nature of the quasi-particle source: coherent or thermal magnon sources are expected to exhibit $g^{(2)}(0)$ values of one or greater, while a value of $g^{(2)}(0)$ smaller than one is the hallmark of a single magnon source.

To compute Eq. (9) explicitly, we reformulate it in terms of the dynamical evolution of the qubit ensemble described by Eq. (2). For $T \rightarrow 0$, the (circularly polarized) transverse fluctuations of the bath spin density (3) can be defined as a response to the magnetic field generated by the qubit array, which reads as

$$\mathbf{h}(\rho, t) = \sqrt{2\tilde{\gamma}} \sum_{\alpha=1}^N \mathcal{D}(\rho_\alpha, \rho, d) \cdot \boldsymbol{\sigma}_\alpha(t). \quad (10)$$

The real-space spin susceptibility χ^{+-} can be obtained by linearizing and Fourier transforming Eq. (4), resulting in the inhomogeneous Helmholtz equation :

$$\left[\nabla^2 + k_0^2 - i\epsilon \right] s^+(\rho, t) = \frac{s\gamma}{D} h^+(\rho, t), \quad (11)$$

with $k_0 = 1/\lambda$ and $\epsilon = \alpha\omega/D$. When considering distances much less than the magnon decay length, Gilbert damping can be neglected, and Eq. (11) can be solved in the far field limit using a Green's function approach, yielding

$$\chi^{+-}(\rho, \rho') = i \sqrt{\frac{1}{8\pi k_0 \rho}} e^{ik_0 \rho} e^{i\frac{\pi}{4}} e^{ik_0 \hat{\rho} \cdot \rho'}, \quad (12)$$

where $\chi^{+-}(\rho, \rho')$ denotes the outgoing plane-wave solution to Eq. (11). Using Eqs. (3), (10), and (12), we can rewrite

$$s^+(\rho, t) = \frac{\gamma \tilde{\gamma} s}{D} \sqrt{\frac{k_0}{8\pi \rho}} e^{-k_0 d} \sum_{\alpha=1}^N e^{ik_0 \hat{\rho} \cdot \rho_\alpha} \sigma_\alpha^+(t), \quad (13)$$

where $\cos^{-1}(\hat{\rho} \cdot \hat{\rho}_\alpha) = \phi$ is the angular position of the detector in the plane of the ferromagnetic film. By plugging Eq. (13) into Eq. (9), the second-order correlation function can be evaluated by numerically solving Eq. (2) [38].

Results.—While our framework applies to an arbitrary number N of magnon emitters, we find that a small number of solid-state spin defects is sufficient to illustrate the salient features of the correlated emission. For

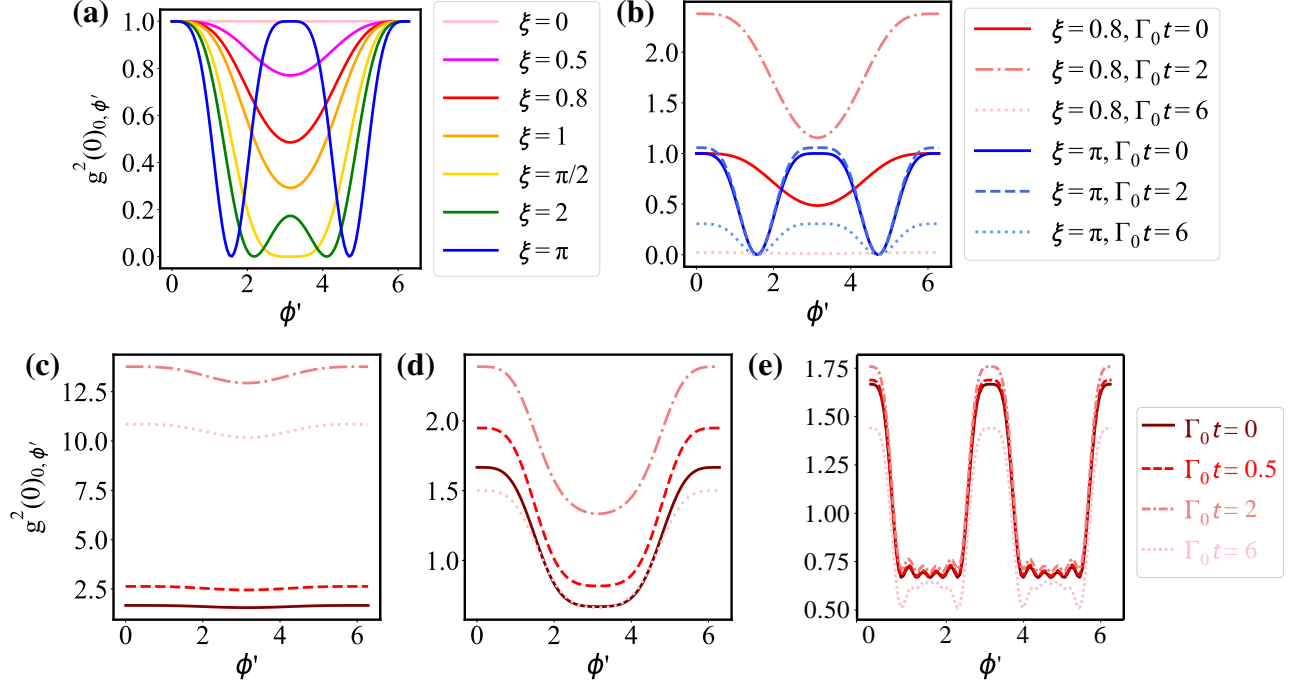


FIG. 2. Dependence of the zero-delay second-order correlation function (14) on the emission angle ϕ' , with fixed $\phi = 0$, for an ensemble of $N = 2$ emitters and different values of ξ : (a) at time $\Gamma_0 t \rightarrow 0$; (b) at various times. Dependence of the zero-delay second-order correlation function (9) on the emission angle ϕ' , with fixed $\phi = 0$, for an ensemble of $N = 6$ emitters at times $\Gamma_0 t = 0$ (solid dark red), $\Gamma_0 t = 0.5$ (dashed red), $\Gamma_0 t = 2$ (dot-dashed light red), and $\Gamma_0 t = 6$ (dotted pink), for (c) $\xi = 0.1$; (d) $\xi = 0.5$; and (e) $\xi = \pi$. In all panels, the parameters correspond to an ensemble of NV-center spins interacting via a YIG thin film, as described in Ref. [18].

$N = 2$, plugging Eq. (13) into Eq. (9) and setting $\tau = 0$ yields the zero-delay correlation function

$$g^{(2)}(0)_{\phi, \phi'} = \frac{(1 + q(\xi, \phi, \phi')) \langle \sigma_1^+ \sigma_2^+ \sigma_1^- \sigma_2^- \rangle}{2 \left| \langle \sigma_1^+ \sigma_1^- \rangle \right|^2}, \quad (14)$$

where $q(\xi, \phi, \phi') = \cos(\xi \cos \phi - \xi \cos \phi')$ and $\xi = k_0 a_q$. The correlators $\langle \sigma_1^+ \sigma_2^+ \sigma_1^- \sigma_2^- \rangle$ and $\langle \sigma_1^+ \sigma_1^- \rangle$ quantify, respectively, the joint transition probability associated with two correlated magnon emissions - one originating from NV_1 and the other from NV_2 - and the probability of two independent magnon emissions.

Figure 2(a) displays the angular dependence of the zero-delay second-order correlation function (14) as a function of the normalized interqubit separation ξ , evaluated in the early-time limit $\Gamma_0 t \rightarrow 0$, where both correlators $\langle \sigma_1^+ \sigma_2^+ \sigma_1^- \sigma_2^- \rangle$ and $\langle \sigma_1^+ \sigma_1^- \rangle$ approach unity. Although no magnons have yet been emitted, $g^{(2)}(0)_{\phi, \phi'}$ captures the angular structure of the joint emission amplitude, governed by interference between spin waves of wavelength λ . In the Dicke limit ($\xi \rightarrow 0$), where the emitters are nearly indistinguishable, the emission becomes fully isotropic, resulting in $g^{(2)}(0) = 1$, independent of direction (red line). As ξ increases, spatial phase differences accumulate between emitters, giving

rise to directional interference effects. In particular, when $\xi(\cos \phi - \cos \phi') = \pi$, destructive interference fully suppresses the joint emission probability, yielding $g^{(2)}(0)_{\phi, \phi'} = 0$.

To investigate the role of the quantum-correlated dynamics of the ensemble, we explore the dynamical evolution of the magnonic correlations (14) for a strongly (weakly) correlated, i.e., $\xi = 0.8$ ($\xi = \pi$) ensemble. As shown in Fig. 2(b), the strongly correlated ensemble exhibits pronounced bunching at early times, followed by a transition to strong anti-bunching at later times. This behavior reflects cooperative dynamics within the array: the initial bunching indicates an enhanced likelihood of simultaneous magnon emission due to collective decay processes, while the subsequent anti-bunching arises from excitation depletion and temporal correlations. In contrast, the correlation function for the weakly correlated ensemble remains nearly unchanged during the evolution, closely resembling the angular structure shown in Fig. 2(a), which indicates that interference predominantly governs its angular dependence.

Finally, we simulate Eq. (2) for an ensemble of $N = 6$ emitters to examine whether the qualitative features identified in the $N = 2$ ensemble persist in larger systems. As in the two-qubit case, signatures of quantum-

correlated dynamics emerge at small inter-emitter spacing. For $\xi = 0.1$, Fig. 2(c) reveals pronounced bunching at early times, indicative of cooperative behavior driven by collective decay. This effect weakens with increasing separation, as shown in Fig. 2(d) for $\xi = 0.5$. In contrast, for $\xi = \pi$, Fig. 2(e) shows that the correlations remain essentially static in time, and the angular structure is dominated by interference, with no evidence of dynamical enhancement in the emission profile.

Discussion and conclusions.—In this work, we identify a regime in which solid-state spin defects coupled to a common magnetic system can serve as a source of both single- and many-body quantum magnonic states. We develop a general framework to characterize the statistics of magnons emitted by the correlated qubit ensemble, which enables us to explore how the signatures of correlated qubit decay are imprinted onto the emitted magnons. Specifically, focusing on a two-qubit setup, we show how the interference between the emitted spin

waves and the quantum correlations of their sources can be probed in the bath via detection measurement. While our analysis focuses on the interactions between solid-state defects and a simple ferromagnet at thermal equilibrium, our framework can be straightforwardly generalized to baths engendering more complex quantum dynamics [34, 39].

Our proposal opens a novel pathway for generating quantum magnonic states and emphasizes the need for future investigations to establish a clear link between the quantum correlations in the collective dynamics of the qubit ensemble and a measurable quantification of entanglement in the emitted magnons.

Acknowledgments.—The authors thank X. Li, J. Marino, and D. Chang for helpful discussions, and E. Foisy for the production of illustrations. B.F. acknowledges support from the ONR under Grant No. N000142412427 and Y.T. acknowledges support from the NSF under Grant No. DMR-2049979.

-
- [1] H. Yuan, Y. Cao, A. Kamra, R. A. Duine, and P. Yan, Quantum magnonics: When magnon spintronics meets quantum information science, *Physics Reports* **965**, 1 (2022), quantum magnonics: When magnon spintronics meets quantum information science.
- [2] B. Flebus, S. M. Rezende, D. Grundler, and A. Barman, Recent advances in magnonics, *Journal of Applied Physics* **133**, 160401 (2023).
- [3] B. F. et al, The 2024 magnonics roadmap, *Journal of Physics: Condensed Matter* (2024).
- [4] S. M. Rezende, *Fundamentals of magnonics*, Vol. 969 (Springer, 2020).
- [5] D. Lachance-Quirion, Y. Tabuchi, A. Gloppe, K. Usami, and Y. Nakamura, Hybrid quantum systems based on magnonics, *Applied Physics Express* **12**, 070101 (2019).
- [6] D. D. Awschalom, C. R. Du, R. He, F. J. Heremans, A. Hoffmann, J. Hou, H. Kurebayashi, Y. Li, L. Liu, V. Novosad, *et al.*, Quantum engineering with hybrid magnonic systems and materials, *IEEE Transactions on Quantum Engineering* **2**, 1 (2021).
- [7] A. V. Chumak, P. Kabos, M. Wu, C. Abert, C. Adelman, A. Adeyeye, J. Åkerman, F. G. Aliev, A. Anane, A. Awad, *et al.*, Advances in magnetics roadmap on spin-wave computing, *IEEE Transactions on Magnetics* **58**, 1 (2022).
- [8] H. Y. Yuan and R. A. Duine, Magnon antibunching in a nanomagnet, *Phys. Rev. B* **102**, 100402 (2020).
- [9] Z. Haghshenasfar and M. G. Cottam, Sub-Poissonian statistics and squeezing of magnons due to the Kerr effect in a hybrid coupled cavity–magnon system, *Journal of Applied Physics* **128**, 033901 (2020).
- [10] J.-k. Xie, S.-l. Ma, and F.-l. Li, Quantum-interference-enhanced magnon blockade in an yttrium-iron-garnet sphere coupled to superconducting circuits, *Phys. Rev. A* **101**, 042331 (2020).
- [11] L. Wang, Z.-X. Yang, Y.-M. Liu, C.-H. Bai, D.-Y. Wang, S. Zhang, and H.-F. Wang, Magnon blockade in a -symmetric-like cavity magnomechanical system, *Annalen der Physik* **532**, 2000028 (2020).
- [12] D. Lachance-Quirion, S. P. Wolski, Y. Tabuchi, S. Kono, K. Usami, and Y. Nakamura, Entanglement-based single-shot detection of a single magnon with a superconducting qubit, *Science* **367**, 425 (2020).
- [13] V. A. S. V. Bittencourt, V. Feulner, and S. V. Kusminskiy, Magnon heralding in cavity optomagnonics, *Phys. Rev. A* **100**, 013810 (2019).
- [14] D. Xu, X.-K. Gu, H.-K. Li, Y.-C. Weng, Y.-P. Wang, J. Li, H. Wang, S.-Y. Zhu, and J. Q. You, Quantum control of a single magnon in a macroscopic spin system, *Phys. Rev. Lett.* **130**, 193603 (2023).
- [15] P. Clausen, D. A. Bozhko, V. I. Vasyuchka, B. Hillebrands, G. A. Melkov, and A. A. Serga, Stimulated thermalization of a parametrically driven magnon gas as a prerequisite for bose-einstein magnon condensation, *Phys. Rev. B* **91**, 220402 (2015).
- [16] C. Du, T. van der Sar, T. X. Zhou, P. Upadhyaya, F. Casola, H. Zhang, M. C. Onbasli, C. A. Ross, R. L. Walsworth, Y. Tserkovnyak, and A. Yacoby, Control and local measurement of the spin chemical potential in a magnetic insulator, *Science* **357**, 195 (2017).
- [17] H. Wang, S. Zhang, N. J. McLaughlin, B. Flebus, M. Huang, Y. Xiao, C. Liu, M. Wu, E. E. Fullerton, Y. Tserkovnyak, and C. R. Du, Noninvasive measurements of spin transport properties of an antiferromagnetic insulator, *Science Advances* **8** (2022).
- [18] X. Li, J. Marino, D. E. Chang, and B. Flebus, *A solid-state platform for cooperative quantum phenomena* (2023).
- [19] D. E. Chang, V. Vuletić, and M. D. Lukin, Quantum nonlinear optics — photon by photon, *Nature Photonics* (2014).
- [20] G. Facchinetti, S. D. Jenkins, and J. Ruostekoski, Storing light with subradiant correlations in arrays of atoms, *Phys. Rev. Lett.* **117**, 243601 (2016).

- [21] A. Asenjo-Garcia, M. Moreno-Cardoner, A. Albrecht, H. J. Kimble, and D. E. Chang, Exponential improvement in photon storage fidelities using subradiance and “selective radiance” in atomic arrays, *Phys. Rev. X* **7**, 031024 (2017).
- [22] V. A. Pivovarov, A. S. Sheremet, L. V. Gerasimov, J. Laurat, and D. V. Kupriyanov, Quantum interface between light and a one-dimensional atomic system, *Phys. Rev. A* **101**, 053858 (2020).
- [23] M. Reitz, C. Sommer, and C. Genes, Cooperative quantum phenomena in light-matter platforms, *PRX Quantum* **3**, 010201 (2022).
- [24] A. Sipahigil, R. E. Evans, D. D. Sukachev, M. J. Burek, J. Borregaard, M. K. Bhaskar, C. T. Nguyen, J. L. Pacheco, H. A. Atikian, C. Meuwly, R. M. Camacho, F. Jelezko, E. Bielejec, H. Park, M. Lončar, and M. D. Lukin, An integrated diamond nanophotonics platform for quantum-optical networks, *Science* **354**, 847 (2016).
- [25] G. J. M. D.F. Walls, *Quantum Optics* (Springer Berlin, Heidelberg, 2008).
- [26] M. B. Plenio and P. L. Knight, The quantum-jump approach to dissipative dynamics in quantum optics, *Rev. Mod. Phys.* **70**, 101 (1998).
- [27] S. Wolf, S. Richter, J. von Zanthier, and F. Schmidt-Kaler, Light of two atoms in free space: Bunching or antibunching?, *Physical review letters* **124**, 063603 (2020).
- [28] K. Y. Guslienko and A. N. Slavin, Magnetostatic green’s functions for the description of spin waves in finite rectangular magnetic dots and stripes, *Journal of Magnetism and Magnetic Materials* **323**, 2418 (2011).
- [29] H. Carmichael, *An Open Systems Approach to Quantum Optics* (Springer-Verlag, 1993).
- [30] F. Casola, T. van der Sar, and A. Yacoby, Probing condensed matter physics with magnetometry based on nitrogen-vacancy centres in diamond, *Nature Reviews Materials* **3** (2018).
- [31] S. J. Masson, I. Ferrier-Barbut, L. A. Orozco, A. Browaeys, and A. Asenjo-Garcia, Many-body signatures of collective decay in atomic chains, *Phys. Rev. Lett.* **125**, 263601 (2020).
- [32] B. Flebus and Y. Tserkovnyak, Quantum-impurity relaxation of magnetization dynamics, *Phys. Rev. Lett.* **121**, 187204 (2018).
- [33] L. Landau and E. Lifshitz, 3 - on the theory of the dispersion of magnetic permeability in ferromagnetic bodies reprinted from *physikalische zeitschrift der sowjetunion* 8, part 2, 153, 1935., in *Perspectives in Theoretical Physics*, edited by L. Pitaevski (Pergamon, Amsterdam, 1992) pp. 51–65.
- [34] X. Li and B. Flebus, *Cooperative non-reciprocal emission and quantum sensing of symmetry breaking* (2024).
- [35] G. S. Agarwal, *Quantum optics* (Cambridge University Press, 2012).
- [36] R. J. Glauber, The quantum theory of optical coherence, *Physical Review* **130**, 2529 (1963).
- [37] E. Sudarshan, Equivalence of semiclassical and quantum mechanical descriptions of statistical light beams, *Physical Review Letters* **10**, 277 (1963).
- [38] J. Johansson, P. Nation, and F. Nori, Qutip 2: A python framework for the dynamics of open quantum systems, *Computer Physics Communications* **184**, 1234 (2013).
- [39] J. M. P. Nair and B. Flebus, *Reservoir-engineered spin squeezing in quantum hybrid solid-state platforms* (2024), arXiv:2410.15588 [quant-ph].